Experimental Validation of the Adams-Welty Model for Heat Transfer in Large-Particle Fluidized Beds

Experimental results for instantaneous and time-averaged local heat transfer coefficients, as well as local voidage and pressure are used to validate the Adams-Welty analytical model of heat transfer to a horizontal cylinder in large-particle fluidized beds. Results support the main assumptions of the model and show that the range of applicability is wider than originally expected.

N. M. CATIPOVIC and T. J. FITZGERALD

Department of Chemical Engineering
Oregon State University
Corvallis, OR 97331

A. H. GEORGE and J. R. WELTY

Department of Mechanical Engineering
Oregon State University
Corvallis, OR 97331

SCOPE

Large-particle fluidized beds have become a topic of considerable interest as a result of the intensive development of fluidized bed coal combustion. There is a lack of reliable heat transfer information for these systems.

Adams and Welty (1979) proposed a gas-convective model for heat transfer to a horizontal cylinder in large-particle beds. Their analysis was the first attempt to predict instantaneous and local heat transfer coefficients under certain fluidizing conditions.

In order to validate the model, an extensive experimental study was conducted. A special instrumented cylinder, designed to make simultaneous measurements of instantaneous local heat transfer rates, voidage, and pressure at several positions on the cylinder surface was used. The objective was to verify the basic assumptions of the Adams-Welty model and to check its range of applicability with regard to particle size, gas velocity and other fluidizing conditions. Experimental work was performed in a cold bed. All components of the model, except the thermal radiation portion, were taken into consideration.

CONCLUSIONS AND SIGNIFICANCE

Good agreement between experimental results and predictions of the Adams-Welty model, over a wide range of fluidizing conditions, support this analytical model derived from first principles. Model predictions of local instantaneous and time-averaged heat transfer coefficients around the circumference of an immersed tube, with and without the presence of gas bubbles, usually differ by less than 15% from experimental values.

Assumptions of the model are shown to be valid for particle diameters greater than 1 mm and particle Reynolds number greater than 50. Although originally derived for the case of a single horizontal tube and gas velocities slightly in excess of U_{mf} (the slow bubble regime), the Adams-Welty model gives satisfactory predictions for tube bundle systems and a wide range of velocities. There is no reason to expect the analysis for the gas convective heat transfer will be any less valid at high bed temperatures. Validation of the thermal radiation portion of the model will require hot bed experiments.

Fluidized beds of large particles ($d_p > 0.5$ mm) have recently become a topic of investigation, primarily as a result of the increasing interest in fluidized bed coal combustion. Combustors typically use dolomite or limestone particles, having diameters greater than 1 mm, to adsorb the sulfur dioxide produced by burning sulfur-containing coal at temperatures of 1,025–1,125 K. The coal makes up only 1–2% of the bed material. Heat is transferred from the bed to an array of immersed horizontal tubes. This energy is utilized for steam generation in electric utility applications and for liquid or gas heating in process industries.

There is a lack of reliable heat transfer data for large-particle beds, which must operate at high gas velocities to be fluidized. Knowledge of heat transfer coefficients to tubes is of great commercial importance since the tubes constitute a significant portion of the total cost of a fluid-bed combustor. In addition to values of

N. M. Čatipović is presently with the Institute for Chemistry, Technology and Metallurgy, Belgrade, Yugoslavia.
T. J. Fitzgerald is with TRW, Inc., Energy Systems Group, Redondo Beach, CA.
A. H. George is with California State University, Chico, CA.
0001-1541-82-6081-0714-$2.00.

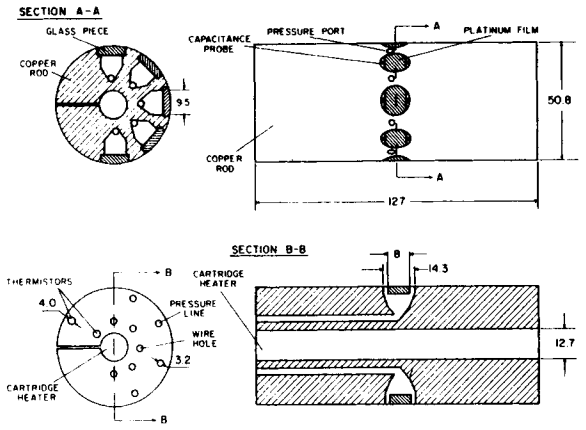

Figure 1. Details of the instrumented cylinder for heat transfer studies (dimensions in mm).

the time-averaged overall heat transfer coefficient, information on temporal and spatial variations of local coefficients is also of interest.

Adams (1977) and Adams and Welty (1979) proposed an analytical model for heat transfer to a horizontal cylinder in large-particle beds. The model considers heat transfer by gas convection to be the dominant mode of energy exchange between an immersed tube and the fluidized bed. The theory is of the type first proposed by Levenspiel and Walton (1954) for bed-to-wall heat transfer. The Adams-Welty model represents the first attempt to analytically predict instantaneous and local heat transfer coefficients under certain fluidizing conditions.

INSTRUMENTATION

Figure 1 shows an instrumented copper cylinder for heat transfer studies. The cylinder was designed to make simultaneous measurements of instantaneous local heat transfer rates, voidage, and pressure at five positions on the cylinder surface.

The heat transfer measuring elements are platinum resistance heaters which are maintained at a constant temperature by an electronic control circuit. Instantaneous heat transfer was obtained by measuring the power required to hold the temperature constant. These rapidly responding elements are inlaid in the copper rod which is maintained at a temperature very close to that of the elements by a cartridge heater and a separate control circuit. On either side of each heat transfer element is a small capacitance probe used to measure the instantaneous voidage in its vicinity. These probes predict bubble passage and enable the calculation of bubble and emulsion residence times on the cylinder surface. Located between the five heat transfer elements are four pressure sensing ports connected to transducers which provide instantaneous static pressure measurements. Details of the instrumentation, with a thorough analysis and examples showing how the various quantities of interest (heat transfer coefficient, voidage, residence time, pressure drop, etc.) are obtained, are given by Čatipović (1979), Čatipović et al. (1978a), and Fitzgerald et al. (1981).

The instrumented cylinder was immersed in a bed having a cross section of 0.48 × 0.125 m. The horizontal axis of the cylinder was located 0.35 m above the distributor plate. Quartz sand and dolomite particles, ranging in from 0.37 to 6.6 mm, were fluidized by air, with the slumped bed height being 0.46 m. Full information on the experimental procedure and physical properties of particles is given by Čatipović (1979). Experiments were performed only under cold bed conditions, at atmospheric pressure.

MAIN ELEMENTS OF THE ADAMS-WELTY MODEL

One of the main assumptions of the Adams-Welty model is that, due to their large thermal inertia, large particles remain essentially

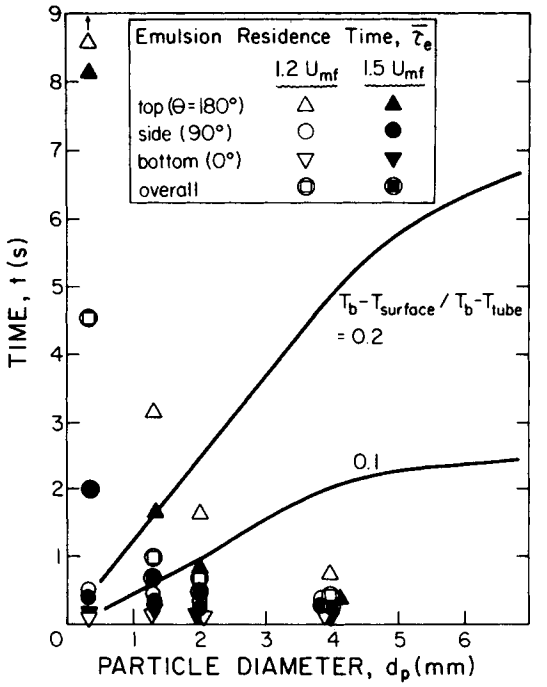

Figure 2. Theoretical curves for transient cooling of a dolomite particle compared with experimental data on particle residence times.

isothermal while in contact with the tube. The authors expected this assumption to be valid for particle diameters greater than 2–3 mm. Figure 2 shows the time required to convectively cool spherical dolomite particles of different diameters, so that the temperature difference between the particle surface and the bed changes by 10% and 20% (curves are from Adams and Welty, 1979). Also shown are some representative particle residence times obtained from experiments. For most fluidizing velocities, it is safe to conclude that, if $d_p > 1$ mm, the change in particle temperature during its contact with the surface can be neglected.

The model takes into account heat transfer resulting from gas flow within interstitial voids adjacent to the tube surface, as well as within bubbles contacting the tube. The interstitial contribution is obtained by an analysis of flow through channels which are bounded below by the tube wall and on the sides by imaginary surfaces which approximately define the domain of circulating gas trapped between neighboring particles. Figure 3 shows the geometry assumed for the interstitial channel. Spacing between particles is determined from the local voidage near the tube surface by the equation

$$\frac{L_c}{d_P} = \frac{0.75}{\sqrt{1-\epsilon_\theta}}$$

A two-dimensional boundary layer flow in the middle portion of the channel and a Stokes-like flow—for which convective terms

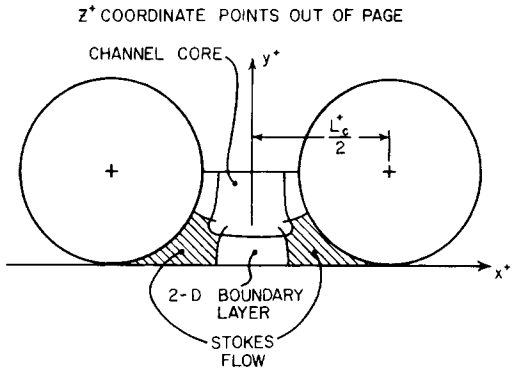

Figure 3. Geometry of interstitial channel.

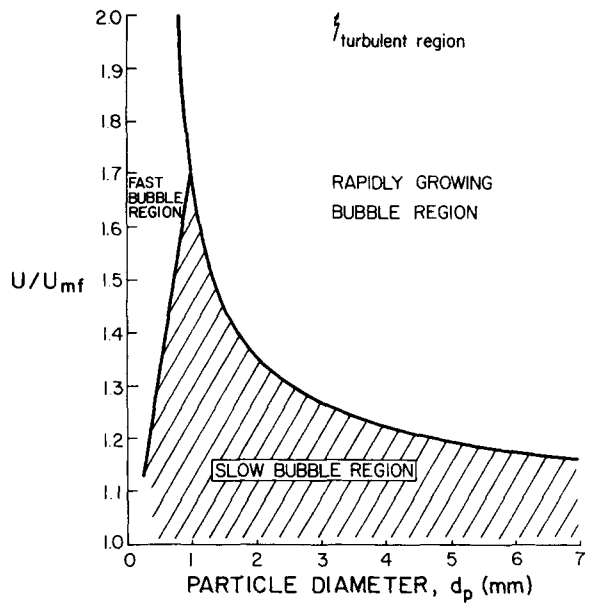

Figure 4. Boundaries of the slow bubble region for dolomite particles, with H_o = 0.46 m.

in the energy equation are neglected—in the cusped corner region, close to the particle contact point, are separately considered. Thermal boundary conditions are: constant temperature at T_{tube} along the tube wall, approximately linear variation from T_{tube} to T_b along the portion of the Stokes' region contacting the particle, and uniform temperature at T_b for the top of the channel, i.e., the free stream for the two-dimensional boundary layer. Interstitial turbulence is incorporated in the two-dimensional boundary layer energy equation. Variation of gas thermal conductivity with temperature is incorporated in the Stokes' region energy equation via the Sutherland formula. The location of the boundary between the Stokes and two-dimensional boundary layer regions is obtained by requiring the Nusselt number be continuous across the channel.

Heat transfer due to thermal radiation and gas convection are assumed to be uncoupled. A relatively simple diffuse-gray enclosure analysis is used to compute the radiative heat transfer. Thermal radiation was not considered in the present study since all experiments were conducted under low-temperature conditions.

Gas velocity in the interstitial channel is assumed to vary linearly along the length of the channel, i.e., stagnation point flow. Determination of the interstitial gas velocity, without bubbles present, by numerical solution of a quasi-steady pressure field equation which accounts for voidage variations in the emulsion phase, is described by George et al. (1979).

Gas convective heat transfer, due to flow within a contacting bubble, is obtained from a two-dimensional boundary layer analysis.

Details of the formulation of both the hydrodynamic and thermal boundary layer portions of the model are given in Adams (1977), Adams and Welty (1979) and George et al. (1979).

Recently, a simplified form of the Adams-Welty model, for heat transfer due to gas flow in interstitial channels, suitable for hand calculations, was developed by Adams (1981). This latest development was not incorporated in the work reported here.

The analysis is limited to a single immersed tube and to slow bubbles. For our experimental conditions, with H_o = 0.46 m, slow bubbles are limited to a region indicated in Figure 4. Its boundaries were obtained from criteria suggested by Čatipović et al. (1978b) and validated experimentally by Jovanovic (1979). The range of applicability of the Adams-Welty model is limited to relatively low values of U/U_{mf}, with the exact limiting value depending on the particle size.

The model is of considerable value because it can predict the effects of changing gas and particle physical properties, bed and tube temperatures, and tube diameter on bed-to-surface heat transfer.

COMPARISON OF EXPERIMENTAL RESULTS WITH MODEL PREDICTIONS

In comparing experimental data with model predictions, it was required that experimental conditions correspond to the situation modeled. For instance, it was found the experimentally determined heat transfer coefficients at minimum fluidization should not be compared against theoretical values because particle residence times, especially on the upper portion of the tube, are such that the assumption of isothermal behavior is no longer valid. Therefore, experimental results used in the comparisons were obtained at velocities which insured adequate particle replacement at the surface.

Comparison of Time-Averaged Local Coefficients

For the case where the emulsion phase covers the entire tube, velocities just slightly in excess of U_{mf} were used. The values used for void fraction, as well as the corresponding physical situation, are shown in Figure 5. The slightly increased voidage on the sides

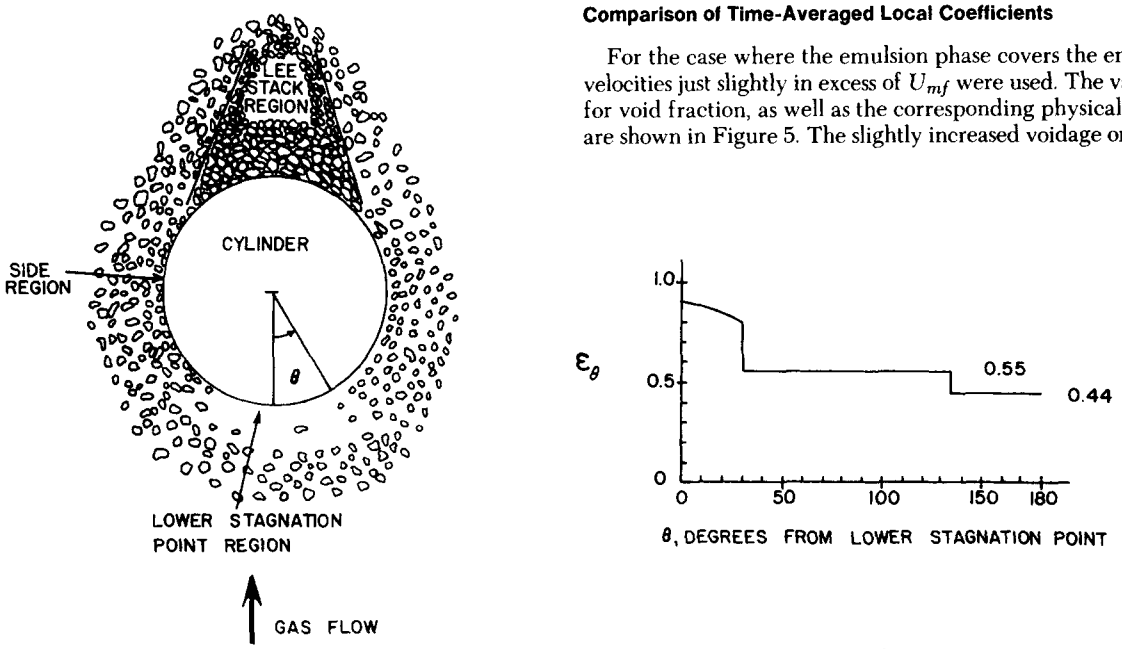

Figure 5. Voidage distribution at the cylinder wall, used in heat transfer modeling.

TABLE 1. GAS VELOCITY AT WHICH THE AVERAGE VOIDAGE AROUND THE TUBE IS 0.57

Particle Diameter d_p (mm)	Superficial Gas Velocity U (m/s)	U/U_{mf}	Re_P
0.37	0.22	1.45	4.58
0.8	0.56	1.22	24.97
1.3	0.77	1.10	56.11
2.0	1.24	1.08	138.16
2.85	1.54	1.06	245.00
4.0	1.90	1.04	426.40
6.6	2.50	1.03	918.60

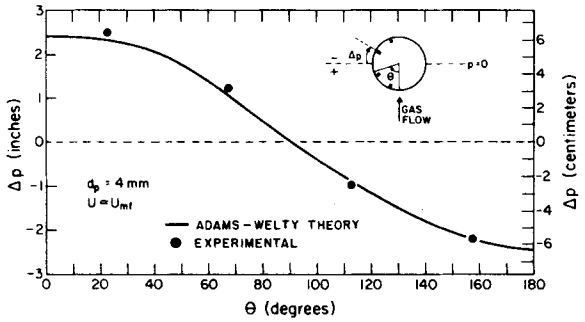

Figure 6. Comparison between predicted and experimental values of time-averaged local pressure drop at cylinder surface for d_p = 4.0 mm (Δp given in cm and inches of water column).

(as compared to ϵ_{mf}) reflects the fact that occasional bubbles pass by the cylinder and insure sufficient particle replacement. The voidage distribution shown essentially represents a time-averaged picture at a velocity slightly above minimum fluidization. Predicted values of local heat transfer coefficients were therefore compared with time-averaged exerimental results.

The average voidage around the tube circumference, resulting from the distribution shown in Figure 5, is 0.57. The gas velocity at which this voidage is measured experimentally depends on the particle size. Table 1 shows the corresponding superficial velocities for the particles used, as well as some other quantities of interest (which will be used in later comparisons).

To validate the hydrodynamic portion of the analytical model, values of time-averaged local pressure at the tube surface were calculated and compared with experimental data. Figure 6, obtained for d_p = 4.0 mm, is representative of the good agreement between predicted and experimental values of local pressure along the cylinder circumference near U_{mf}, for particle diameters above 1 mm.

The pressure calculation, as well as other procedures (interstitial velocity determination, heat transfer solution for the lower stagnation point region, assessment of the influence of interstitial turbulence, etc.) are described in detail by Adams (1977) and George et al. (1979).

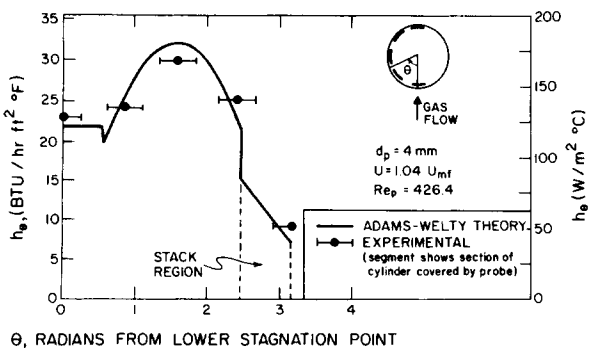

Figure 7. Comparison between theoretical and measured values of local heat transfer coefficients for d_p = 4.0 mm.

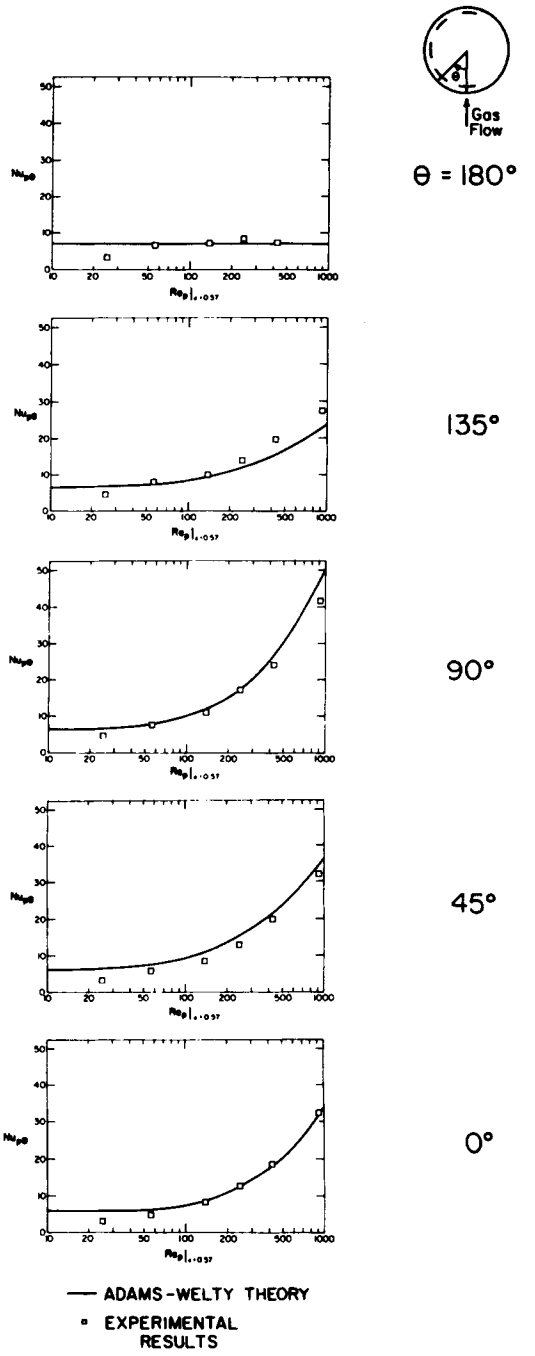

Figure 8. Comparison between theoretical and measured values of local Nusselt numbers for particles used in this study. (See Table 1).

In the heat transfer comparisons which follow, the value of the interstitial turbulence intensity in the model was set at $u' = 0.2$, as suggested by experiments of Galloway and Sage (1970) for large spherical particles.

Figure 7 shows a typical comparison between theoretical and measured values of local heat transfer coefficients. For a more meaningful comparison, the theoretical coefficients were averaged over the section of the cylinder covered by the platinum sensor. Figure 8 shows a detailed graphical summary of this type of comparison for particles used in our experiments. The graphs are plotted in terms of dimensionless groups $Nu_{p\theta}$ and Re_p since such representation provides a convenient way of assessing the influence of physical properties on heat transfer behavior.

The agreement between experiment and theory is very satisfactory, both in values and trends, supporting the basis of the analytical model. Under the operating conditions considered here, the lower limit of the model's applicability seems to be around 1

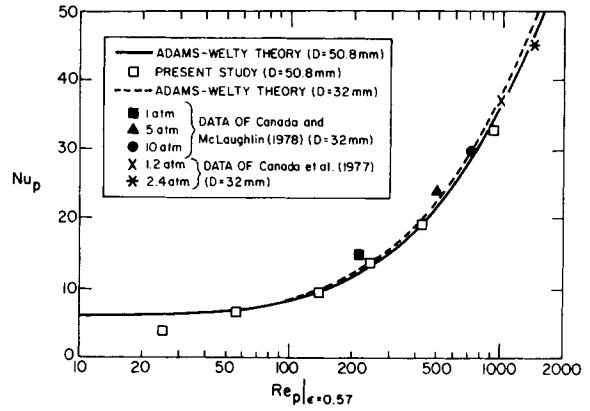

Figure 9. Comparison between theoretical and measured values of the overall Nusselt number for three different studies.

mm (Re_p = 50); this significantly exceeds Adams and Welty's conservative estimate of 2–3 mm. As particle diameter decreases below 1 mm, the disagreement between predictions and data becomes significant, reaching 1504–200% for 0.37 mm particles (not shown in Figure 8). The thermal inertia of smaller particles is not sufficient to keep them isothermal while at the tube wall; therefore, the actual heat transfer coefficient is well below predicted. It must be noted that the actual limit of the model will depend on the physical properties of gas and particles.

Actual and predicted local heat transfer coefficients shown in Figure 8 rarely differ by more than 15%. At present, these are the only data available for the local coefficients.

The agreement is even more striking when overall coefficients are considered. Figure 9 compares theory versus experiment for three cases: a) data of this study using a 50.8 mm cylinder at atmospheric pressure, with air as the fluidizing gas; b) data of Canada and McLaughlin (1978) using a 32 mm tube in a bed of 2.6 mm glass particles, with air at three different pressures; and c) data of Canada et al. (1977) using the same setup as in b), but with Freon-12 at 1.2 and 2.3 atm. The heat transfer coefficients used for comparison in cases b) and c) are those obtained at 1.1 U_{mf}.

The model is successful in predicting the effect of gas properties on heat transfer. It also correctly predicts the negligible influence of tube diameter. For fine particles Gelperin et al. (1969) suggested that heat transfer coefficients are independent of the tube diameter for tube diameters greater than 20 mm. No such information has been previously reported for large particles.

Comparison of Instantaneous Local Coefficients in the Presence of Bubbles

The Adams-Welty model can predict instantaneous local heat transfer coefficients for practically any configuration of a single bubble clinging to the immersed cylinder. In order to obtain data for comparison with these predictions, superficial gas velocities slightly higher than in the previous section were used.

Plexiglas inserts were placed in the bed to reduce its thickness to 50 mm. In such a narrow bed, bubbles could be seen easily. When in operation, this two-dimensional bed was backlighted and filmed with a Nikon R-10 camera at 18 frames per second. For every frame registered on film, the corresponding heat transfer, voidage, and pressure signals were registered on a Data General Nova 840 computer. These data gave instantaneous values of local heat transfer rates, voidage, and pressure which correspond to the picture on the film frame.

Several hundred movie frames were examined, and the corresponding predicted and experimental values were compared. In all of the simulations, the voidage distribution was as shown in Figure 5, except that the voidage on the sides of the tube was taken as 0.5. As in the comparison of time-averaged values, the model gave good predictions for particle diameters of 1.3 mm and larger, with the agreement getting better as particle size increased. Predicted and measured values of instantaneous local heat transfer coefficients rarely differed by more than 15%, while the instantaneous average values for the entire circumference agreed to within 10%. Some illustrative examples are given in the figures which follow.

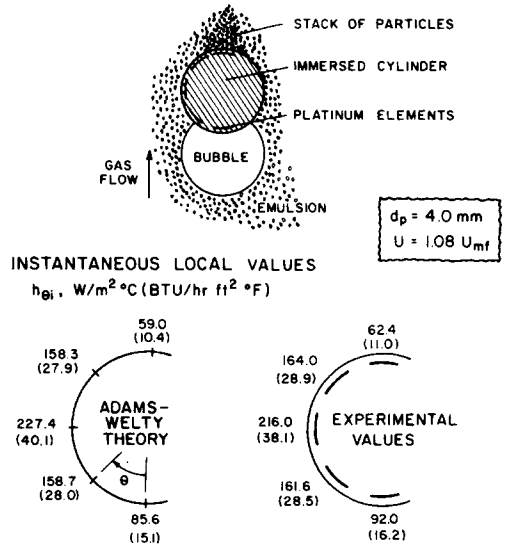

Figure 10. Comparison between theoretical and measured values of instantaneous local heat transfer coefficients for bubble configuration shown (d_p = 4.0 mm, narrow bed).

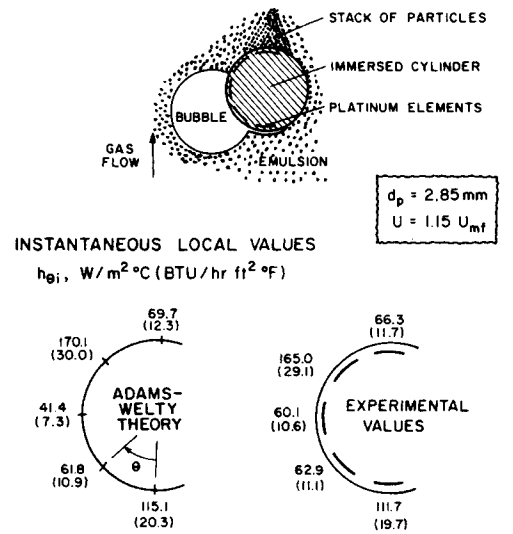

Figure 11. Comparison between theoretical and measured values of instantaneous local heat transfer coefficients for bubble configuration shown (d_p = 2.85 mm, narrow bed).

Figure 10 illustrates the good agreement between local heat transfer coefficients for the case of a bubble engulfing the bottom platinum sensor (d_p = 4.0 mm), while Figure 11 compares prediction vs. experiment for a bubble clinging to the side of the cylinder (d_p = 2.85 mm). These comparisons were made for the narrow, two-dimensional bed. Several other cases are given in Čatipović (1979).

The numerous cases with different bubble positions cannot all be presented. However, experimental data confirm the success of the Adams-Welty model in predicting the influence of bubble location on instantaneous local heat transfer coefficient for particle diameters above 1 mm.

COMMENTS

An apparent disadvantage of the Adams-Welty model is that it is applicable only for a narrow range of ratios U/U_{mf}. However,

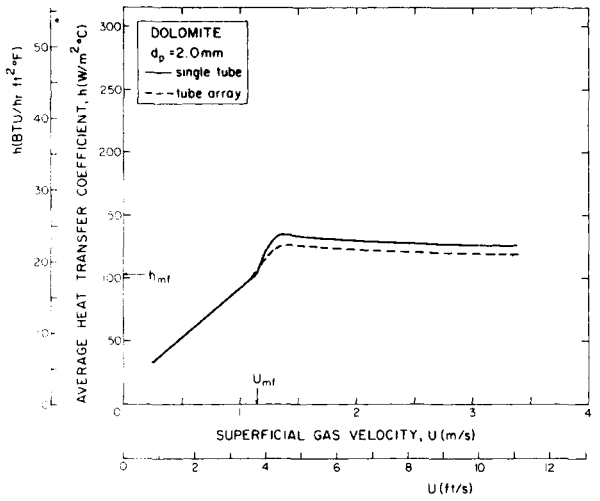

Figure 12. Time-averaged overall heat transfer coefficient as a function of gas velocity, for d_p = 2.0 mm.

the model could prove to be useful for predictions of the time-averaged overall heat transfer coefficient in large-particle beds in general since coefficients slightly above U_{mf} appear to represent good first approximations for heat transfer at higher velocities. This is certainly the case for $d_p > 0.5$ mm at room temperature and atmospheric pressure (Čatipović, 1979; Chandran et al., 1980). Figure 12 (Čatipović, 1979) is a representative illustration.

Figure 12 also shows a surprisingly small difference between the heat transfer coefficient for a single tube and that of closely-spaced tube array (pitch/diameter = 2). This appears to be generally true for pitch/diameter ratios ≥ 2, as shown by Čatipović (1979) and Chandran et al. (1980) for large particles, and Gelperin et al. (1969) for fine particle systems. The data of Canada et al. (1977) and Canada and McLaughlin (1978), which are compared with model prediction in Figure 9, were for a tube bundle.

CONCLUSIONS

The Adams-Welty model has been verified for cold bed conditions. Experimental evidence, over a broad range of fluidizing conditions, supports this analytical model derived from first principles. The model is also successful in predicting the effect of gas properties on heat transfer. There is no reason to expect that the analysis for the gas convective heat transfer will be any less valid at high bed temperatures and pressures (the latter being of particular interest for dual-cycle utility applications) provided the particle Reynolds number is greater than about 50. Validation of the thermal radiation portion of the model will require experimental work at high temperatures. For most practical purposes, the model gives satisfactory predictions for tube bundle systems and a wide range of fluidizing velocities.

ACKNOWLEDGMENT

Experimental work was part of a research and development program sponsored by the Electric Power Research Institute, while the theoretical work was prepared, in part, for the United States Department of Energy under Contract No. EF-77-S-01-2714.

NOTATION

D = diameter of immersed tube (cylinder), m or mm
d_p = diameter of particle, m or mm
H_o = slumped bed height, m
h = time-averaged heat transfer coefficient for the entire tube (time-averaged overall coefficient), W/m²·K
h_θ = time-averaged local heat transfer coefficient at angular position θ, W/m²·K
$h_{\theta i}$ = instantaneous local heat transfer coefficient at angular position θ, W/m²·K
k_g = gas thermal conductivity at bed temperature, W/m·K
L_c = channel length (particle center-to-center spacing), m or mm
L_c^+ = L_c/D
Nu_p = $\left(= \frac{hd_p}{k_g}\right)$ = time-averaged overall Nusselt number based on particle diameter
$\mathrm{Nu}_{p\theta}$ = $\left(= \frac{h_\theta d_p}{k_g}\right)$ = time-averaged local Nusselt number based on particle diameter
fP = pressure, cm H_2O (Pa)
Re_p = $\left(= \frac{U\rho_g d_p}{\mu_g}\right)$ = Reynolds number based on particle diameter and gas properties at bed temperature
T = temperature, K
t = time, s
U = superficial gas velocity, m/s
x^+, y^+, z^+ = x/D, y/D, z/D; coordinates

Greek Letters

ϵ_θ = local voidage at angular position θ
θ = angle on the tube surface measured from the lower stagnation point, radians or degrees
$\bar{\tau}_e$ = overall average emulsion residence time, s
μ_g = gas viscosity at bed temperature, Pa·s
ρ_g = gas density at bed temperature and pressure, kg/m³

Subscripts

b = fluidized bed
mf = at minimum fluidization
surface = particle surface
tube = tube (cylinder)

LITERATURE CITED

Adams, R. L., "An Analytical Model of Heat Transfer to a Horizontal Cylinder Immersed in a Gas Fluidized Bed," Ph.D. Thesis, Oregon State University, Corvallis, OR (1977).

Adams, R. L., "An Approximate Formula for Gas Convection Heat Transfer in Large-Particle Fluidized Beds," *J. Heat Transfer*, in press (1981).

Adams, R. L., and J. R. Welty, "A Gas Convection Model of Heat Transfer in Large Particle Fluidized Beds," *AIChE J.*, **25**, 395 (1979).

Canada, G. S., and H. H. McLaughlin, "Large Particle Fluidization and Heat Transfer at High Pressures," *AIChE Symp. Ser.*, **74** (176), 27 (1978).

Canada, G. S., M. H. McLaughlin, and F. W. Staub, "Two-Phase Flow and Heat Transfer in Fluidized Beds," Eighth and Ninth Quarterly Reports, prepared for the Electric Power Research Institute (Contract RP 525-1), SRD-77-110 and SRD-77-150, General Electric Corporate Research and Development, Schenectady, NY (1977).

Čatipović, N. M., "Heat Transfer to Horizontal Tubes in Fluidized Beds: Experiment and Theory," Ph.D. Thesis, Oregon State University, Corvallis, OR (1979).

Čatipović, N. M., T. J. Fitzgerald, and G. N. Jovanovic, "A Study of Heat Transfer to Immersed Tubes in Fluidized Beds," Paper 28e, AIChE 71st Annual Meeting, Miami Beach, FL (1978a).

Čatipović, N. M., T. J. Fitzgerald, and G. N. Jovanovic, "Regimes of Fluidization for Large Particles," *AIChE J.*, **24**, 543 (1978b).

Chandran, R., J. C. Chen, and F. W. Staub, "Local Heat Transfer Coefficients Around Horizontal Tubes in Fluidized Beds," *J. Heat Transfer*, **102**, 152 (1980).

Fitzgerald, T. J., N. M. Catipović, and G. N. Jovanovic, "An Instrumented Cylinder for Studying Heat Transfer to Immersed Tubes in Fluidized Beds," *Ind. Eng. Chem. Fund.*, **20**, 82 (1981).
Galloway, T. R., and B. H. Sage, "A Model of the Mechanism of Transport in Packed, Distended, and Fluidized Beds," *Chem. Eng. Sci.*, **25**, 495 (1970).
Gelperin, N. I., V. G. Ainshtein, and L. A. Korotyanskaya, "Heat Transfer Between a Fluidized Bed and Staggered Bundles of Horizontal Tubes," *Int. Chem. Eng.*, **9**, 137 (1969).
George, A. H., N. M. Čatipović, and J. R. Welty, "An Analytical Study of Heat Transfer to a Horizontal Cylinder in a Large Particle Fluidized Bed," ASME Paper No. 79-HT-78, ASME-AIChE 18th National Heat Transfer Conference, San Diego, CA (1979).
Jovanovic, G., "Gas Flow in Fluidized Beds of Large Particles: Experiment and Theory," Ph.D. Thesis, Oregon State University, Corvallis, OR (1979).
Levenspiel, O., and J. S. Walton, "Bed-Wall Heat Transfer in Fluidized Systems," *Chem. Eng. Prog. Symp. Ser.*, **50** (9), 1 (1954).

Manuscript received July 30, 1980; revision received September 14 and accepted October 9, 1981.

Distribution for Maximum Activity of a Composite Catalyst

D. B. DADYBURJOR
Department of Chemical and Environmental Engineering
Rensselaer Polytechnic Institute
Troy, NY 12181

For a catalyst composed of a more active component embedded in a less active (but not inert) and more diffuse matrix, an optimum distribution of the active component in the catalyst pellet may lead to significantly higher reaction rates per unit volume of pellet, compared with reaction rates using pellets with a uniformly distributed active component or with an active component concentrated on the outside or the inside of the pellet. The optimum distribution changes qualitatively with the physical parameters of the pellet and with changes in the rate constants and diffusion coefficients of the catalytic components. This is relevant to the performance of coking zeolite/silica-alumina catalysts in hydrocarbon cracking reactions.

SCOPE

Catalysts used for the cracking of petroleum fractions consist of particles of rare-earth exchanged zeolite (crystalline aluminosilicate) embedded in a matrix of amorphous silica-alumina. The activity of the zeolite component towards cracking is greater than that of the matrix, but the resistance to diffusion is significantly lower in the matrix than in the zeolite. Such composite catalysts appear to have a higher activity and improved resistance to coking than either constituent used separately.

Ruckenstein (1970) showed that embedding an active catalyst uniformly in a more porous but inactive solid could significantly increase the reaction rate over that if the catalyst only was present. Varghese and Wolf (1980) showed that a uniformly distributed composite catalyst had significant advantages over an undiluted catalyst under conditions of pore mouth poisoning.

It is of interest to consider whether a nonuniform distribution of active component in a porous matrix offers any advantages over a uniform distribution, particularly where the matrix itself is also catalytically active, albeit to a small extent. Further, if the catalyst is coked while it is on stream, the reaction rate constants and diffusion resistance of both components are altered. Hence the optimum distribution is different from that of a fresh catalyst. The objectives of the present paper are to obtain the overall reaction rates for a composite catalyst containing a reactive matrix with different distributions of the more active component, and to obtain optimum distributions for a number of changes in reaction constants, diffusion coefficients, and sizes, of the constituents.

CONCLUSIONS AND SIGNIFICANCE

The overall reaction rate is obtained for a composite catalyst pellet of infinite flat plate geometry, with the more active component also present as flat plates (strata) but of lesser thickness. This geometry leads to a significant ease in analysis with little loss of rigor. Nominal values of parameters used are of the order of those expected in catalytic cracking using zeolite/silica-alumina catalysts.

For the simple case of a uniform distribution of the more active component, increasing the size of the composite catalyst decreases the reaction rate per unit volume of composite, as expected. Two special cases of nonuniform distribution are considered, where the more active component is isolated either at the external surface or at the center of the composite catalyst. The conformation with the more active component in the center is found to be more reactive than the conformation where the more active component is at the surface. This is shown to be a consequence of the non-zero catalytic activity of the matrix. The uniformly distributed catalyst possesses a higher activity than either of the two extreme distributions, except when the size is sufficiently small that diffusional limitations can be ignored. There all three cases tend to the same asymptotic value.

An attempt is made to simulate the effect of coking by decreasing the rate constant of the more active component and the diffusion coefficient of the matrix. As the properties of the matrix and the more active component decrease, so does the